11-30-2017

An optical method for carbon dioxide isotopes and mole fractions in small gas samples: Tracing microbial respiration from soil, litter, and lignin

Steven J. Hall
Iowa State University, stevenjh@iastate.edu

Wenjuan Huang
Iowa State University, wjhuang@iastate.edu

Kenneth E. Hammel
U.S. Department of Agriculture

An optical method for carbon dioxide isotopes and mole fractions in small gas samples: Tracing microbial respiration from soil, litter, and lignin

Abstract

Rationale

Carbon dioxide isotope (δ13C value) measurements enable quantification of the sources of soil microbial respiration, thus informing ecosystem C dynamics. Tunable diode lasers (TDLs) can precisely measure CO2 isotopes at low cost and high throughput, but are seldom used for small samples (≤5 mL). We developed a TDL method for CO2 mole fraction ([CO2]) and δ13C analysis of soil microcosms.

Methods

Peaks in infrared absorbance following constant volume sample injection to a carrier were used to independently measure [12CO2] and [13CO2] for subsequent calculation of δ13C values. Using parallel soil incubations receiving differing C substrates, we partitioned respiration from three sources using mixing models: native soil organic matter (SOM), added litter, and synthetic lignin containing a 13C label at Cβ of the propyl side chain.

Results

Once-daily TDL calibration enabled accurate quantification of δ13C values and [CO2] compared with isotope ratio mass spectrometry (IRMS), with long-term external precision of 0.17 and 0.31‰ for 5 and 1 mL samples, respectively, and linear response between 400 and 5000 μmol mol−1CO2. Production of CO2 from native soil C, added litter, and lignin Cβ varied over four orders of magnitude. Multiple-pool first-order decay models fitted to data (R2 > 0.98) indicated substantially slower turnover for lignin Cβ (17 years) than for the dominant pool of litter (1.3 years) and primed soil C (3.9 years).

Conclusions

Our TDL method provides a flexible, precise, and high-throughput (60 samples h−1) alternative to IRMS for small samples. This enables the use of C isotopes in increasingly sophisticated experiments to test biogeochemical controversies, such as the fate of lignins in soil.

Disciplines

Biogeochemistry | Ecology and Evolutionary Biology | Soil Science

Comments

This article is published as Hall, Steven J., Wenjuan Huang, and Kenneth E. Hammel. "An optical method for carbon dioxide isotopes and mole fractions in small gas samples: Tracing microbial respiration from soil, litter, and lignin." *Rapid Communications in Mass Spectrometry* 31, no. 22 (2017): 1938-1946. doi: 10.1002/rcm.7973.

Received: 27 June 2017 | Revised: 21 August 2017 | Accepted: 23 August 2017

DOI: 10.1002/rcm.7973

WILEY Rapid Communications in Mass Spectrometry

RESEARCH ARTICLE

An optical method for carbon dioxide isotopes and mole fractions in small gas samples: Tracing microbial respiration from soil, litter, and lignin

Steven J. Hall[1] | Wenjuan Huang[1] | Kenneth E. Hammel[2,3]

[1] Department of Ecology, Evolution, and Organismal Biology, Iowa State University, 251 Bessey Hall, Ames, IA 50011, USA

[2] US Forest Products Laboratory, Madison, WI 53726, USA

[3] Department of Bacteriology, University of Wisconsin, Madison, WI 53706, USA

Correspondence
S. J. Hall, Department of Ecology, Evolution, and Organismal Biology, Iowa State University, 251 Bessey Hall, Ames, IA 50011, USA.
Email: stevenjh@iastate.edu

Funding information
Directorate for Biological Sciences, Grant/Award Number: 1457805; National Science Foundation, Grant/Award Number: 1331841

Rationale: Carbon dioxide isotope ($\delta^{13}C$ value) measurements enable quantification of the sources of soil microbial respiration, thus informing ecosystem C dynamics. Tunable diode lasers (TDLs) can precisely measure CO_2 isotopes at low cost and high throughput, but are seldom used for small samples (≤5 mL). We developed a TDL method for CO_2 mole fraction ($[CO_2]$) and $\delta^{13}C$ analysis of soil microcosms.

Methods: Peaks in infrared absorbance following constant volume sample injection to a carrier were used to independently measure $[^{12}CO_2]$ and $[^{13}CO_2]$ for subsequent calculation of $\delta^{13}C$ values. Using parallel soil incubations receiving differing C substrates, we partitioned respiration from three sources using mixing models: native soil organic matter (SOM), added litter, and synthetic lignin containing a ^{13}C label at C_β of the propyl side chain.

Results: Once-daily TDL calibration enabled accurate quantification of $\delta^{13}C$ values and $[CO_2]$ compared with isotope ratio mass spectrometry (IRMS), with long-term external precision of 0.17 and 0.31‰ for 5 and 1 mL samples, respectively, and linear response between 400 and 5000 μmol mol^{-1} CO_2. Production of CO_2 from native soil C, added litter, and lignin C_β varied over four orders of magnitude. Multiple-pool first-order decay models fitted to data ($R^2 > 0.98$) indicated substantially slower turnover for lignin C_β (17 years) than for the dominant pool of litter (1.3 years) and primed soil C (3.9 years).

Conclusions: Our TDL method provides a flexible, precise, and high-throughput (60 samples h^{-1}) alternative to IRMS for small samples. This enables the use of C isotopes in increasingly sophisticated experiments to test biogeochemical controversies, such as the fate of lignins in soil.

1 | INTRODUCTION

Tunable diode laser (TDL) absorption spectrometry is a powerful technique for measuring carbon dioxide mole fraction ($[CO_2]$) and stable isotope ratios ($\delta^{13}C$ and/or $\delta^{18}O$ values). The relatively low cost, rapid measurement speed, and analytical simplicity of TDL technology present new opportunities for routine isotope measurements in biogeochemical studies. Although TDL methods are increasingly used to measure CO_2 dynamics in the field,[1-4] they have rarely been applied to the analysis of small gas samples[5,6] which are typical of laboratory microcosm studies. Application of TDLs to incubation experiments could enable increasingly sophisticated and high-resolution experiments to improve our understanding of biogeochemical processes, by exploiting variation in natural abundance $\delta^{13}C$ values as well as using ^{13}C-labeled substrates. Here, we built on recent work[6] to optimize a TDL method for small gas samples. We illustrate the sensitivity and capabilities of this method with an experiment where we assessed the decomposition of litter, soil organic matter (SOM), and lignin with a site-specific ^{13}C label.

Tunable diode lasers require a continuous flow of analyte gas through the instrument, which normally demands sample volumes of hundreds of mL to L to purge the system and achieve measurement stability.[1,7] This design is appropriate for atmospheric analyses where sample volumes are not limiting, as well as for closed-loop applications where sample gas is re-circulated through the instrument. However, logistical constraints often require the analysis of much smaller sample volumes (mL). These include situations where low respiration rates preclude continuous measurements of CO_2 fluxes; where collection of larger gas samples can disturb the system of interest; or, in field environments where deployment of a TDL is unfeasible.

Recent studies introduced TDL methods to measure $\delta^{13}C$ values of CO_2 in small gas samples but these have not yet been effectively coupled with TDL measurements of $[CO_2]$ to enable simultaneous calculation of soil respiration. Engel et al[5] analyzed headspace gas flushed from incubation chambers using CO_2-free air to quantify the $\delta^{13}C$ values of invertebrate respiration with a TDL. Subsequently, Moyes et al[6] demonstrated that small gas samples (<5 mL) could be directly injected into a TDL via a carrier gas to achieve $\delta^{13}C$ measurements with comparable precision (0.25‰) to continuous flow IRMS. However, this method required the analysis of a consistent CO_2 molar quantity for each sample, thus requiring separate analyses for $[CO_2]$ and $\delta^{13}C$ values.

Here, we developed and validated a high-throughput TDL method(~60 samples h^{-1}) for the simultaneous measurement of $\delta^{13}C$ values and $[CO_2]$ in small (1 and 5 mL) air samples spanning a wide concentration range (100–5000 μmol mol^{-1} CO_2). We illustrate the potential insights obtainable from frequent $\delta^{13}C$ measurements of soil respiration using an experiment where CO_2 production was partitioned among SOM, added leaf litter, and added lignin with a site-specific ^{13}C label. Lignin is a major and chemically complex constituent of higher plants that resists biodegradation and shields cellulose and hemicellulose from enzymatic attack. As a consequence, lignin is generally thought to constrain rates of plant litter decomposition over timescales of months to years.[8,9] However, the ultimate importance of lignin as a constituent of SOM remains controversial. It was long thought that lignin derivatives were major constituents of slow-cycling SOM, which persisted due to their relative biochemical recalcitrance.[10] Recent work challenged this paradigm by suggesting that lignin is not preferentially retained during long-term (years to decades) decomposition.[11-13] Yet, other work suggests that methodological constraints may have inadvertently obscured the contributions of lignin to SOM, due to the preferential association of lignin with reactive minerals.[14,15] Conventional assays of lignin (e.g., cupric oxide oxidation) appear to systematically underestimate lignin content in mineral soils.[15]

Isotope-labeled synthetic lignins offer a promising but underutilized tool to quantitatively probe the biogeochemical dynamics of lignin, by providing a tracer that can be quantitatively recovered in the gas or solid phase. Seminal work by Kirk et al[16] and Haider and colleagues[17-19] demonstrated the utility of lignins prepared with ^{14}C labels at specific atoms within the lignin polymer to investigate controls on lignin decay. Analytical advances since that original work now permit the use of a ^{13}C label as opposed to ^{14}C, enhancing the precision of the method.[20]

Isotope-labeled lignins can be synthesized in the laboratory using biochemical precursors and oxidative enzymes in processes analogous to those occurring during natural lignin biosynthesis in plant tissues.[16] Early work demonstrated that synthetic lignins and lignins produced *in planta* decompose at similar rates.[17] These data and detailed spectroscopic analyses confirmed that the synthetic lignins were biologically realistic.[21,22] However, synthetic lignins offer a clear analytical advantage because lignins isolated from plant material inevitably contain polysaccharide impurities and, if the lignins have been isotope-labeled *in planta*, some of the label also appears in these polysaccharides.[21] Contamination of isotope-labeled lignins with a small fraction of isotope-labeled polysaccharides can lead to spurious results, as their mineralization rates can differ by an order of magnitude or more.[19]

Our objectives were as follows: (1) develop a precise and high-throughput TDL method for the measurement of $\delta^{13}C$ values and $[CO_2]$; and (2) apply the method to a microcosm experiment to partition respiration contributions from SOM, added litter, and synthetic lignin as a proof of concept.

2 | EXPERIMENTAL

2.1 | Sample analysis

We measured the $\delta^{13}C$ values of CO_2 and $[CO_2]$ using a tunable diode laser absorption spectrometer (TGA200A; Campbell Scientific, Logan, UT, USA). The operating principles of a similar instrument were previously described in detail by Bowling et al.[7] The instrument used here contains a thermoelectrically cooled interband cascade laser instead of a cryogenically cooled lead salt diode laser. The TGA200A independently measured $[^{12}CO_2]$ and $[^{13}CO_2]$ by absorption at wavelengths of 4348.5 and 4348.2 nm, respectively. The sample flow rate was 50 mL min^{-1}, the detector temperature was −5°C, and the pressure was 2 kPa. A Nafion drier removed water vapor. The gap between the laser and lens of the TGA was purged with ultra-high-purity nitrogen (10 mL min^{-1}). The TGA sample inlet was connected to ultra-zero grade CO_2-free air used as a carrier gas. To maintain a constant carrier flow through the TGA, excess zero air (>10 mL min^{-1} relative to the TGA sample flow) was purged through a manifold upstream of a mass flow controller. A reference gas (produced in our lab as described below; 2008 ppm CO_2 in air, $\delta^{13}C$ = −9.90‰ relative to VPDB) was analyzed concurrently with samples to maintain laser spectral alignment and provide initial estimates of sample $[^{12}CO_2]$ and $[^{13}CO_2]$.

Individual gas samples were injected into the carrier gas through a rubber septum housed in a brass T fitting. Polypropylene syringes (5 mL; Becton-Dickinson, Franklin Lakes, NJ, USA) with Luer stopcocks and 25-gauge needles were used for sample injections. We analyzed eight standards to produce calibration curves for $[^{12}CO_2]$ and $[^{13}CO_2]$, used to calculate $[CO_2]$ and $\delta^{13}C$ values during post-processing. Four standard tanks (~400 to 850 μmol CO_2 mol^{-1}) were prepared at the University of Utah Stable Isotope Ratio Facility for Environmental Research (SIRFER; Salt Lake City, UT, USA) by diluting concentrated CO_2 from sources with differing $\delta^{13}C$ values in compressed ambient air. These tanks were calibrated at SIRFER relative to World Meteorological Organization (Geneva, Switzerland) primary standards (X2007 CO_2 scale). The $\delta^{13}C$ values of CO_2 on the IAEA VPDB scale were measured using a dual-inlet isotope ratio mass spectrometer (DeltaPlus Advantage; ThermoFinnigan, Bremen, Germany), and $[CO_2]$ was measured with an infrared gas analyzer (LI-7000; LiCor, Lincoln, NE, USA). Additional standard tanks were prepared at Iowa State University, Ames, IA, USA (ISU) by diluting ultra-pure CO_2 in compressed ambient air, and/or by mixing with the tanks described above. For these latter tanks, the $\delta^{13}C$ value of CO_2 was measured using another continuous flow isotope ratio mass

spectrometer at ISU (DeltaPlus XL; ThermoFinnigan), and [CO_2] was measured by gas chromatography (GC, 2014A gas chromatograph; Shimadzu, Columbia, MD, USA) using a thermal conductivity detector. Measurements of [CO_2] by GC at ISU were independently calibrated using four *separate* NIST-traceable standards with [CO_2] between 400 and 5000 μmol mol^{-1}. Overall, the [CO_2] of the standard gases used in this study ranged from 117 to 5233 μmol mol^{-1}, with $\delta^{13}C$ values of CO_2 from −4.45‰ to −14.31‰. We note that these standard gases can in principle be used to calibrate the $\delta^{13}C$ values of CO_2 from samples spanning a much broader range of δ values, because [$^{13}CO_2$] and [$^{12}CO_2$] are measured and calibrated *independently* via the TDL.[23] Thus, the only analytical requirement for a given sample is that [$^{13}CO_2$] and [$^{12}CO_2$], as opposed to the $\delta^{13}C$ value, should be bracketed by the range of measured standards. This contrasts with IRMS methods where isotope ratios are measured explicitly.

2.2 | Data processing

Ten-Hz measurements of [$^{12}CO_2$] and [$^{13}CO_2$] were recorded on a datalogger (CR3000; Campbell Scientific) along with instrument diagnostic parameters. The 1-Hz mean values were used for subsequent peak identification and calibration in R,[24] as demonstrated in the example code in the supporting information. (The file 'Metadata_for_TDL_data.docx' provides an overall description of the data files. The file 'TDL_data.csv' is raw data from the TGA200A recorded by the datalogger as described above. The file 'sample_names.csv' is the sequential list of gas standards and samples as they were injected into the TGA200A. The file 'TDL_CO2_analysis_demo_script.docx' is code that can be run using R software[24] to identify CO_2 peaks from raw data, to name them using the sample list, and to generate calibrated $\delta^{13}C$ and [CO_2] values using the identified standards.)

Air samples injected into the TGA produced approximately Gaussian peaks for [$^{12}CO_2$] and [$^{13}CO_2$] (Figure 1). Maximum values of [$^{12}CO_2$] and [$^{13}CO_2$] corresponding to individual sample peaks were identified in the time series. Regressions between measured peak heights and known mole fractions of standards were used to generate separate calibration curves for [$^{12}CO_2$] and [$^{13}CO_2$]. Peak heights rather than areas were used because of the ambiguity in consistently defining the area of peaks with long tails. Preliminary observations showed that using 1-Hz mean data as opposed to 10-Hz raw data yielded greater reproducibility of calibrated $\delta^{13}C$ values over time. The relationships between peak heights and CO_2 mole fractions were linear across the range of standards used here (~100 to 5000 μmol mol^{-1}), and including a second-order polynomial term in the calibration regression equation did not significantly improve the fit of the linear models ($p > 0.05$). The peak height–mole fraction relationships became nonlinear for [$^{12}CO_2$] above approximately 6000 μmol mol^{-1} (data not shown). Calibrated values for [$^{12}CO_2$] and [$^{13}CO_2$] were converted into $\delta^{13}C$ values following the convention:[25] $\delta^{13}C = \frac{R_{sample}}{R_{standard}} - 1$, where R is the molar ratio of $^{13}C/^{12}C$ and VPDB is the standard.

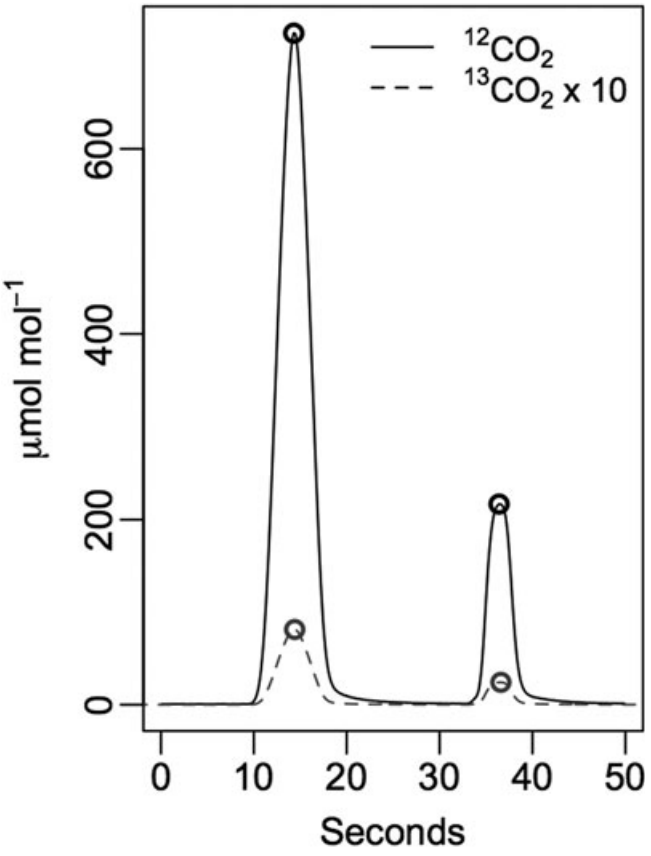

FIGURE 1 Peaks for $^{12}CO_2$ and $^{13}CO_2$ measured on the TGA200A following injection of 5- and 1-mL samples of a standard gas (720.8 μmol mol^{-1} CO_2), respectively. The trace for $^{13}CO_2$ was multiplied 10-fold for clarity. Circles represent peak heights (local maxima) used to independently calibrate $^{12}CO_2$ and $^{13}CO_2$ for calculations of $\delta^{13}C$ values and [CO_2] during post-processing

2.3 | Assessment of precision and temporal stability

During the incubation experiment described below, standard curves for [$^{12}CO_2$] and [$^{13}CO_2$] were measured on each sampling date by injecting each of the eight standards five times in series. We calculated multiple standard curves for each date that sequentially omitted one standard, allowing us to treat each standard as an unknown to characterize precision and accuracy. The standard with greatest [CO_2] (5233 μmol mol^{-1}) was not treated as an unknown, as it would have fallen well outside the range of the remaining standards. During sample analyses, we analyzed an additional standard in triplicate as an unknown following every 10 samples to characterize precision.

2.4 | Soil incubation experiment

Surface soil (0–10 cm) was collected from the Luquillo Experimental Forest, Puerto Rico, for incubation experiments. This ecosystem is a montane, per-humid tropical forest with mean annual precipitation of 3800 mm $year^{-1}$ and temperature of 24°C, and is described in detail elsewhere.[26] The soil is a clay-rich Oxisol formed from volcaniclastic sediments with C and N content of 34.1 and 3.0 mg g^{-1}, respectively. Soil was passed through an 8-mm sieve to remove coarse roots while retaining micro-aggregate structure. Replicate 1-g soil subsamples

(dry mass equivalent) were used for incubations at field moisture capacity (~1 g H_2O g soil^{-1}). Three treatments were established: (1) soils were incubated alone (control); (2) soils were amended with 100 mg C_4 litter + synthetic lignin; (3) soils were amended with 100 mg C_4 litter + synthetic lignin labeled with 99 atom% ^{13}C at the C_β position of each lignin C_9 substructure ($^{13}C_\beta$-labeled lignin). Scission of the lignin polymer is required for the release of C_β; thus mineralization of C_β to CO_2 is a conservative diagnostic of lignin degradation. Syntheses of the high molecular weight ^{13}C-labeled and natural abundance lignins and their characterization with nuclear magnetic resonance (NMR) spectroscopy are described elsewhere.[22] The litter consisted of oven-dried and ground *Andropogon gerardii* (big bluestem, a C_4 grass) leaf tissue harvested after shortly after senescence (41.3% C, 1.1% N). We precipitated synthetic lignins on the *A. gerardii* litter in a 1:20 mass ratio by dissolving lignins in a 4:1 solution of acetone and water, thoroughly mixing the solution with the ground litter, and evaporating the acetone/water solution at 40°C.[21] The average phenylpropane structure in $^{13}C_\beta$ lignin has a molecular mass of 197,[22] so the ^{13}C label represented 13/197 of the added synthetic lignin mass. The litter/lignin mixtures were gently homogenized with soil samples and brought to field moisture capacity with deionized water.

The samples were incubated at 23°C in glass jars (946 mL) sealed with Viton gaskets and aluminum lids, which were equipped with butyl septa for headspace gas sampling via a syringe and needle. The jars were maintained sealed during the experiment and flushed with CO_2-free air after each headspace measurement, allowing cumulative quantification of mineralized CO_2 and $\delta^{13}C$ over time. The jars were stored in the dark between measurements. Blank jars (without soil) were similarly analyzed to assess background contamination. To further validate [CO_2] measured by the TGA200A with GC, a subset of headspace gas samples (n = 610) was analyzed by both methods, as described above. These samples had [CO_2] between 25 and 1634 μmol mol^{-1}, measured by GC.

2.5 | Source partitioning of CO_2 and rate constant modeling

The $\delta^{13}C$ values of soil and the added C_4 litter were −27.6‰ and −12.7‰, respectively, determined by combustion to CO_2 on an elemental analyzer (Costech, Valencia, CA, USA) in line with the DeltaPlus XL isotope ratio mass spectrometer at ISU (described above). We used mixing models to partition CO_2 production from soil, litter, and synthetic lignin as follows. The $\delta^{13}C$ values of CO_2 produced from the control soils (no litter added) were used as end members for soil-respired CO_2. We used −10.7‰ as the end member for C_4-litter-derived CO_2 to account for the fact that carbohydrates have $\delta^{13}C$ values ~2‰ greater than those of bulk leaf tissue,[25] and assuming that most CO_2 production from litter would derive from carbohydrates over timescales of weeks to months.[8,9] The fractional contributions of added litter and native SOM to soil respiration were partitioned using a two-source mixing model and measurements from the litter + unlabeled lignin treatment. This was expressed in atom fraction ^{13}C notation for increased precision:

$$f_{litter} = \frac{x(^{13}C)_{soil+litter} - x(^{13}C)_{soil}}{x(^{13}C)_{litter} - x(^{13}C)_{soil}}$$

Here, $x(^{13}C)_{soil+litter}$ is the measured atom fraction of $^{13}CO_2$, produced from soil with C_4 litter and unlabeled synthetic lignin; $x(^{13}C)_{soil}$ is the measured atom fraction of $^{13}CO_2$, from the soil alone; $x(^{13}C)_{litter}$ is defined *a priori* as described above. Mineralization of the synthetic lignins accounted for <1% of total soil respiration and thus the impact of *unlabeled* synthetic lignin on the $\delta^{13}C$ value of the respired CO_2 can be neglected. Rather, inclusion of the unlabeled lignin along with the C_4 litter provides a control to account for any inhibitory effects of the added synthetic lignin on litter decomposition. We then calculated the contribution of the $^{13}C_\beta$-labeled lignin to soil respiration using a mixing model with the litter + $^{13}C_\beta$ lignin and litter + unlabeled lignin treatments as end members:

$$f_{lignin} = \frac{x(^{13}C)_{soil+litter+13C\ lignin} - x(^{13}C)_{soil+litter}}{x(^{13}C)_{lignin} - x(^{13}C)_{soil+litter}}$$

Here $x(^{13}C)_{soil+litter+13C\ lignin}$ is the measured atom fraction of $^{13}CO_2$ from the incubation of soil and C_4 litter with $^{13}C_\beta$-labeled lignin and $x(^{13}C)_{soil+litter}$ is as described above; $x(^{13}C)_{lignin}$ is 0.99 for C_β. Production of CO_2 derived from soil, litter, and lignin $^{13}C_\beta$ was calculated by multiplying the total measured CO_2 flux from the soil + litter treatments by the fractional contributions of CO_2 as calculated above. We calculated the cumulative fraction of C mass remaining from soil, litter, and lignin, $^{13}C_\beta$, over time to estimate decomposition constants from multiple-pool first-order models fitted by nonlinear least squares using the 'nls' function in R. For each component, we used Akaike's Information Criterion to select the optimum among one-, two-, and three-pool models.

3 | RESULTS

3.1 | Effects of injection volume on [CO_2] and $\delta^{13}C$ measurement

Injections of 1- and 5-mL samples into the carrier gas produced symmetrical peaks that declined to baseline within 20–30 s, depending on [CO_2] (Figure 1). The relationships of $^{12}CO_2$ and $^{13}CO_2$ peak heights with known mole fractions depended on the sample injection volume (Figure 2). For both 5-mL and 1-mL injections of standard gases, the respective peak heights of $^{12}CO_2$ and $^{13}CO_2$ showed a very strong linear relationship with their known mole fractions (R^2 = 1.000 for all four lines) across the entire range of values (Figure 2). The slopes of the regression lines between peak heights and CO_2 mole fractions differed between injection volumes (Figure 2), indicating the need to apply separate calibration curves for each volume injected. For example, applying the calibration curves produced from 5-mL injections to 1-mL injections with similar peak heights overestimated the mean CO_2 mole fractions by 47%, probably as a consequence of differing peak shape as a function of injection volume.

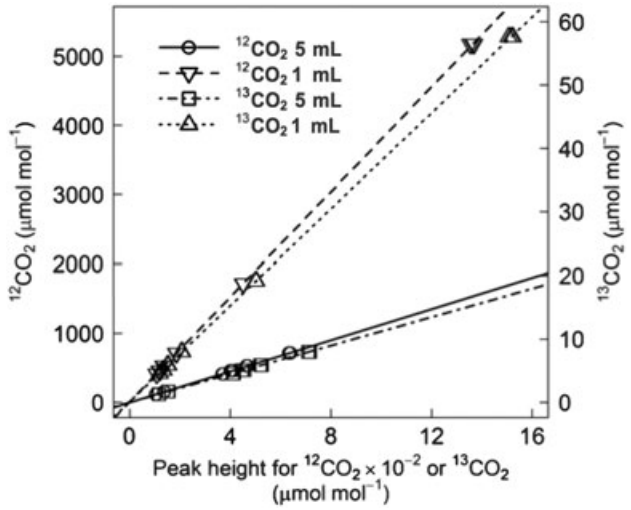

FIGURE 2 Relationships between the peak heights of $^{12}CO_2$ and $^{13}CO_2$ and the known values. The solid line is the linear regression line for $^{12}CO_2$ measurements from 5-mL injections: $y = 1.13x - 2.07$. The dashed line is for $^{12}CO_2$ measurements from 1-mL injections: $y = 3.79\,x + 7.02$. The dot-dashed line is for $^{13}CO_2$ measurements from 5-mL injections: $y = 1.12\,x - 0.02$. The dotted line is for $^{13}CO_2$ measurements from 1-mL injections: $y = 3.79x + 0.09$

3.2 | Method performance over time

We sequentially measured each standard as an unknown on each measurement date, using the remaining standards for calibration. The $\delta^{13}C$ values of each of the seven standards showed no significant directional drift ($p > 0.05$, $R^2 < 0.12$ for all standards) during the 129-day measurement period, assessed by linear regressions between $\delta^{13}C$ values and sampling date (Figure 3A). For 5-mL samples, the long-term $\delta^{13}C$ precision (one σ standard deviation) was 0.20, 0.14, 0.17, 0.23, and 0.10‰ for standards with $[CO_2]$ between 415 and 1758 μmol mol^{-1} (Figure 3A). Neither the precision nor the accuracy of the $\delta^{13}C$ values of these standards significantly varied as a function of $[CO_2]$. However, the standards with very low $[CO_2]$ (117 and 155 μmol mol^{-1}) were much more variable over time, with $\delta^{13}C$ precisions of 0.91‰ and 0.72‰, respectively (Figure 3B). Changing the order in which standards were analyzed had no effect on the measured $\delta^{13}C$ values, implying the absence of a significant 'memory effect'.

The $\delta^{13}C$ values for 5-mL injections were significantly more precise (t test, $p < 0.0001$) than those of the 1-mL injections from the same standards. The precision of the 1-mL standards with $[CO_2]$ between 415 and 1758 μmol mol^{-1} measured 0.36, 0.28, 0.28, 0.24, and 0.41‰. The mean long-term standard deviation of all 5-mL standards was 0.17‰, compared with 0.31‰ for the 1-mL injections. The method was highly accurate in terms of reproducing the known $\delta^{13}C$ value of each standard when the standards were analyzed as unknowns on each sampling date. The average (±SD) difference between the measured and known $\delta^{13}C$ values was −0.03 ± 0.11 and 0.03 ± 0.14 for the 1- and 5-mL injections, respectively. Overall, the $[CO_2]$ measured by the TGA agreed very well with that measured by GC ($R^2 = 0.999$), which was calibrated by an independent set of standards. However, the slope of the regression line (0.995 ± 0.001) was slightly but significantly different from 1 ($p < 0.001$) due to the high statistical power of the analysis. Measurements of $[CO_2]$ were similarly precise for both 1- and 5-mL sample injection volumes, with long-term mean relative standard deviations (RSDs) of 0.9 ± 0.4 and 0.7 ± 0.4%, respectively.

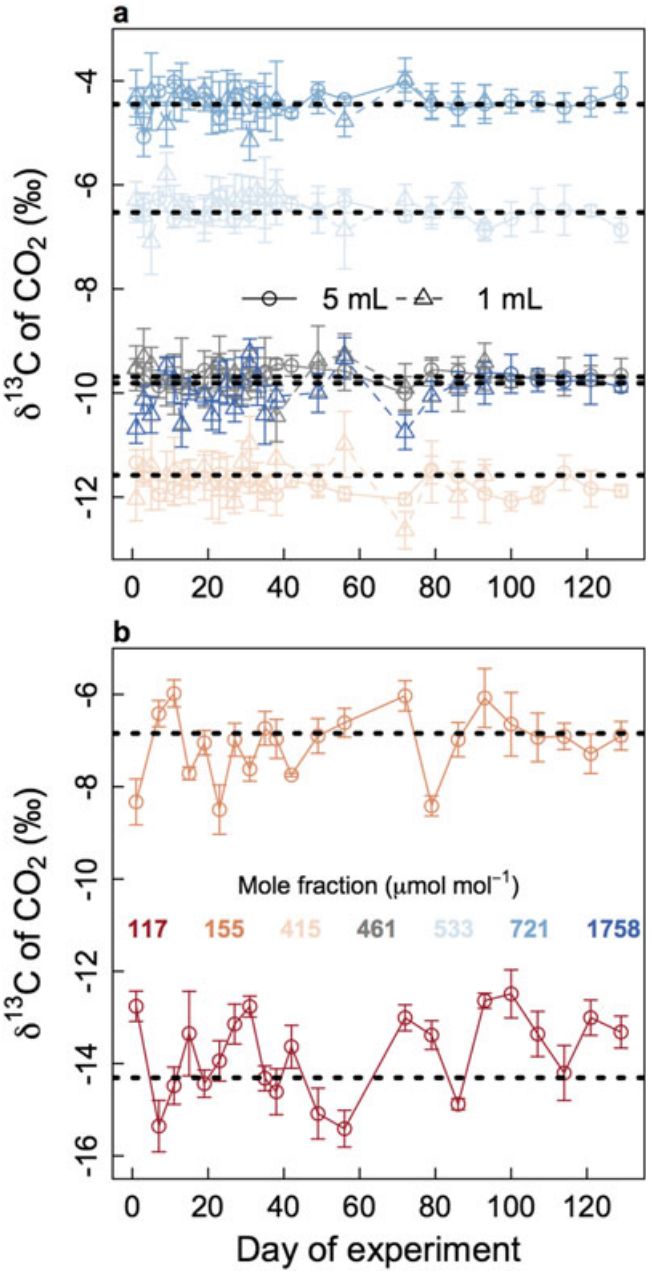

FIGURE 3 Values of $\delta^{13}CO_2$ in standards measured as unknowns over a period of 129 days, with 1- and 5-mL injections denoted by triangles and circles, respectively. Colors indicate CO_2 mole fractions for each time standard (117–1758 μmol mol^{-1}) as indicated in the legend, from red (lower concentration) to tan-grey (intermediate) to blue (higher concentration). The dotted lines indicate the known $\delta^{13}CO_2$ values for each standard. Standards with $[CO_2]$ <400 μmol mol^{-1} had greater variability and are shown in B [Color figure can be viewed at wileyonlinelibrary.com]

To assess the need for daily calibration, we used a calibration curve from the first day of measurement to calculate the $\delta^{13}C$ values of the standard gases over the rest of the experiment. The $\delta^{13}C$ measurements were less accurate and precise without daily calibration: measured values differed between 0.24‰ and 1.03‰ of known values, and long-term standard deviations varied between 0.31‰ and

1.16‰. To assess the need for high-frequency calibration to correct for instrument drift, we analyzed a check standard three times following every 10 samples. The average variability within each set of three replicates (0.31‰) was typically similar to the overall variability of the check standards analyzed on a given date (0.30‰), and there was no evidence of consistent directional drift in $\delta^{13}C$ values over timescales of hours. Thus, following analysis of the initial calibration curve, we elected not to drift-correct the data within a given sampling date.

3.3 | $\delta^{13}C$ values of respired CO_2 and source partitioning

Given the increased precision in the $\delta^{13}C$ values of the 5-mL vs 1-mL sample injections, we report 5-mL data from the soil incubation experiment. The $\delta^{13}C$ values of respired CO_2 differed substantially among soil incubation treatments (Figures 4A and 4B), enabling partitioning of soil, litter, and lignin contributions to soil respiration and their cumulative fluxes over time (Figure 4C). The respiration $\delta^{13}C$ values from the soil-only treatment were −18.3 ± 1.4‰ at the beginning of the experiment and increased consistently for 16 days, and subsequently oscillated around −27.6‰, the $\delta^{13}C$ value of bulk soil organic C (Figure 4A). The CO_2 flux-weighted $\delta^{13}C$ value of soil respiration was −27.4‰ (calculated as the average $\delta^{13}C$ value over the experiment weighted by CO_2 production at each measurement point). In the litter + lignin treatment, the $\delta^{13}C$ values of the soil respiration initially measured −12.8 ± 0.2‰ and decreased over the following 16 days to −14.8 ± 0.9‰, before increasing to −12.0 ± 1.0‰ at 36 days (Figure 4A). After this point, the $\delta^{13}C$ values declined linearly (R^2 = 0.72, $p < 0.0001$) over the remainder of the experiment, yielding an overall flux-weighted $\delta^{13}C$ value of −13.8‰. In the litter + labeled lignin treatment, the $\delta^{13}C$ value of the soil respiration initially measured −3.6 ± 1.0‰ and increased to 18.8 ± 2.0‰ over 16 days. Subsequently, the $\delta^{13}C$ values gradually decreased and remained stable near 10‰ over the following 50 days. At approximately 76 days, the $\delta^{13}C$ values began a linear increase (R^2 = 0.90, $p < 0.0001$) that continued over the next 50 days.

The contributions of SOM, litter, and the $^{13}C_\beta$ moiety of lignin to soil respiration in the litter + lignin treatments varied by approximately four orders of magnitude (Figure 4C). Litter was a dominant but variable component of respiration, accounting for 66–88% of total CO_2 production over the course of the experiment. After 36 days, the contribution of litter declined steadily (R^2 = 0.71, $p < 0.0001$) for the remainder of the experiment, balanced by a concomitant increase in contributions from SOM, which accounted for 29 ± 6.0% of CO_2 production by the end of the experiment. The production of CO_2 from both litter and SOM declined over time for the first 20 days, but litter CO_2 production subsequently increased between 20 and 40 days. After 40 days, CO_2 production from litter declined, while CO_2 production from SOM remained relatively stable.

3.4 | Statistical models of C turnover

Multiple-pool first-order decay models closely reproduced the observed C mineralization from litter, soil, and lignin, with R^2 values between 0.979 and 0.999 (Table 1; Figure 4D). Litter C

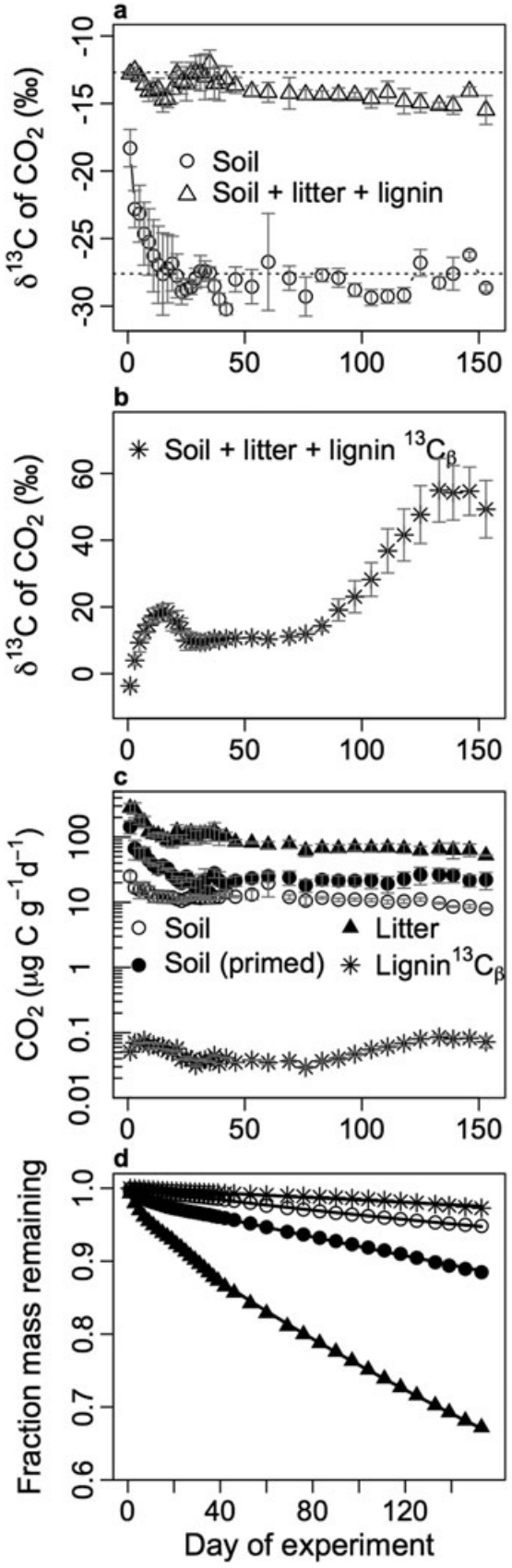

FIGURE 4 Temporal trends in $\delta^{13}C$ values of CO_2 from soil incubation treatments (A, B), contributions of litter, SOM, and lignin $^{13}C_\beta$ to respiration (C), and cumulative mass loss and model fits indicated by lines (D). Error bars are standard errors (n = 3), but are not included in (D) for clarity. Soil (primed) denotes CO_2 production from SOM in the treatment that received added litter

TABLE 1 Parameters for first-order decay models fit to C mass loss data partitioned by $\delta^{13}C$ measurements and mixing models

Component	f_1	k_1	T_1 (years)	f_2	k_2	T_2 (years)	f_3	k_3	T_3	R^2
Litter	0.01 (0.01)	182.1 (80.45)	0.01	0.05 (0.01)	10.9 (80.5)	0.09	0.94 (0.01)	0.79 (0.03)	1.27	0.999
Lignin C_β	1	0.06 (0)	16.7	--	--	--	--	--	--	0.979
SOM (primed)	0.01 (0)	81.2 (9.07)	0.01	0.99 (0)	0.26 (0)	3.85	--	--	--	0.999
SOM	0.16 (0.71)	0.95 (2.31)	1.05	0.84 (0.71)	0 (0.37)	--	--	--	--	0.999

f, k, and T indicate the fractional contribution of each pool to total C, the decomposition rate constant of that pool, and the mean turnover time, respectively. The optimum model (one, two, or three pools) was selected by AIC. SOM (primed) refers to C loss from SOM in the litter addition treatment. Standard errors (n = 3) are shown in parentheses.

mineralization was best explained by a three-pool model, where small fractions of litter C (0.01 and 0.05) had mean turnover times of days and weeks, and the largest fraction of C (0.94) had a mean turnover time of 15 months. The combination of high R^2 values with relatively high standard errors of model parameters indicated considerable statistical flexibility in partitioning C among the three pools in the model (Table 1). Lignin $^{13}C_\beta$ mineralization was best described by a one-pool model with a mean turnover time of about 17 years. Soil C mineralization in the litter + lignin treatment was best described with a two-pool model, where a very small C fraction (0.01) had a turnover time of days, and most soil C (0.99) had a mean turnover time of 4 years. Soil C mineralization in the treatment that did not receive litter addition decomposed more slowly. In the optimum model, most C decomposed by zero-order kinetics (k = 0; independent of C mass), and a small fraction (0.16) had a turnover time of 1 year.

4 | DISCUSSION

4.1 | Method performance

Dual-inlet or continuous flow IRMS have long been the standard methods for the measurement of the $\delta^{13}C$ values of CO_2 for soil biogeochemical studies. The precision for dual-inlet IRMS can be as high as 0.01‰,[28] and is slightly lower (0.05–0.2‰) for continuous-flow IRMS.[29,30] A previous TDL method for the measurement of small gas samples achieved reasonable precision,[6] but required injection of a consistent CO_2 mole quantity for each sample. Our method, based on independent measurement of the $[^{12}CO_2]$ and $[^{13}CO_2]$ peak heights rather than their ratios, achieved similar precision to Moyes et al,[6] but enabled relatively precise simultaneous measurements of $\delta^{13}C$ values and $[CO_2]$ across a much wider range of mole fractions (~400 to 5000 μmol mol^{-1}). The analytical variability in our method was greater at sub-ambient CO_2 mole fractions (~100 to 150 μmol mol^{-1}), probably due to decreased signal relative to background noise (Figure 3), but this constraint can often be avoided in incubation studies by extending sample incubation times to generate increased CO_2 mole fractions. Cavity ring-down spectroscopy is another analytical technique amenable to the analysis of moderate sample sizes (30 mL), and can potentially achieve reasonable precision (0.30‰) for the $\delta^{13}C$ value of CO_2.[31] However, the sophisticated spectral analysis algorithms of some instruments using this technology preclude direct user calibration in terms of the peak heights of individual $[^{12}CO_2]$ and $[^{13}CO_2]$ absorption lines as described here (e.g., Figures 1 and 2), and these instruments are potentially vulnerable to alignment issues that cannot be addressed by the user.

4.2 | Trends in natural abundance $\delta^{13}C$ values of CO_2 over time

Comparatively few studies have measured the $\delta^{13}C$ value of soil respiration CO_2 at natural abundance during prolonged soil incubations.[32] The degree to which the $\delta^{13}C$ value of respired CO_2 reflects the $\delta^{13}C$ values of organic substrates and bulk soil C remains contested, and the degree to which fractionation may occur during heterotrophic metabolism remains an important uncertainty for interpreting natural abundance $\delta^{13}C$ measurements.[33] Fewer studies have conducted $\delta^{13}C$ measurements of soil respiration with sufficient frequency to precisely quantify the mass-weighted $\delta^{13}C$ flux of soil respiration during extended incubations. Recent work has provided some evidence for decoupling between the $\delta^{13}C$ values of CO_2 and bulk soil C,[29,34-37] but these experiments generally relied on less frequent sampling or did not calculate $\delta^{13}C$ fluxes weighted by cumulative CO_2 production. Here, we found that the cumulative $\delta^{13}C$ values of CO_2 from controls (soil alone) were equivalent to the $\delta^{13}C$ values of bulk soil C, despite a short period of increased $\delta^{13}C$ values early in the experiment (Figure 4A). This early period of increased $\delta^{13}C$ values may reflect disturbance and the respiration of labile compounds and microbial biomass, both of which are typically enriched in the heavy isotope relative to bulk soil C.[27,33] Our comprehensive data support the hypothesis proposed by Ehleringer et al[33] and subsequent work:[32,38] soil heterotrophic respiration does not necessarily impart a significant kinetic isotope fractionation

4.3 | Decomposition rate constants for SOM, litter, and lignin $^{13}C_\beta$

Frequent measurements of $\delta^{13}C$ values and $[CO_2]$ allowed us to fit first-order decay models that closely approximated trends in mass loss (Figure 4D), with much greater R^2 than typically accomplished using relatively infrequent (i.e., weekly or monthly) IRMS measurements.[39] Mass loss trends for the added litter were well described by a three-pool model, and the overall mass-weighted mean litter turnover time (1.2 years) was relatively similar to the mean turnover times of leaf litter from several species (0.8 year) calculated from a field litterbag experiment at this site,[40] and the incubation temperature was very similar to the site mean annual temperature. A two-pool model fitted

native soil C loss in soils with added litter quite well (Table 1). However, the ~4-year mean turnover time derived from these data probably masked the presence of slower cycling pools that could not be readily discerned over this relatively short-term incubation.[41] In contrast to litter and SOM, lignin $^{13}C_{\beta}$ decomposed much more slowly, and was best described by a single-pool model with a mean turnover time of 17 years.

Notably, the turnover of lignin $^{13}C_{\beta}$ was similar to the mean turnover times (11–26 years) of the 'slow' pool that accounts for ~2/3 of mineral-associated C in this soil as determined by rigorous measurements of ^{14}C in contemporary and 25-year-old archived samples,[42] and this is slightly slower than the mean turnover of lignin methoxyls (13 years) examined previously in this soil.[43] Slower turnover of lignin C_{β} than of methoxyl C presumably reflects the differing recalcitrance of these moieties, as methoxyl C is readily released from the lignin polymer by nonselective oxidants such as the Fenton reagent[44] and the resulting one-carbon moieties (methanol, formaldehyde, or formic acid) are readily biodegraded. The CO_2 production from lignin C_{β} showed greater temporal variation than did CO_2 from added litter or SOM, with two prominent peaks of increased $^{13}C_{\beta}$ mineralization (Figure 4C). This may reflect the importance of microbial community dynamics in governing lignin depolymerization, given that a relatively narrow suite of microbes have been demonstrated to generate the strong, non-specific oxidants that mediate this process.[45]

5 | CONCLUSIONS

Our TDL injection method enabled precise, high-throughput (~60 samples h^{-1}) measurement of $\delta^{13}C$ values and mole fractions of CO_2 in 5-mL gas samples spanning 400–5000 μmol mol^{-1}. The data from our soil incubation case study provided an important counterpoint to recent biogeochemical syntheses, which have proposed that biochemical recalcitrance has little impact on organic matter turnover.[11-13] In contrast, we found that lignin C_{β} turnover was markedly slower than that of bulk litter or bulk SOM, and was of similar magnitude to the dominant pool of mineral-associated C in this soil. How important might lignin be as a constituent of decadal-cycling SOM pools, and how important are biological and geochemical factors in mediating these dynamics? Given the demonstrated biases in conventional cupric oxide lignin assays,[15] experiments combining TDL analyses with additions of ^{13}C-labeled lignins and other substrates provide a promising way forward to address ongoing controversies of the dynamics of SOM.

ACKNOWLDEGEMENTS

We thank two anonymous reviewers for detailed comments that improved the manuscript. We are indebted to M. Garcia for careful preparation of CO_2 standards at SIRFER, and to D. Bowling for mentorship of SJH and for commenting on a draft of this manuscript. We thank S. Ankerstjerne and A. Wanamaker for assistance with IRMS analyses at Iowa State, and L. Reyes and L. Mack for lab assistance. Funding was provided by NSF grant DEB-1457805 and the NSF Luquillo Critical Zone Observatory.

ORCID

Steven J. Hall http://orcid.org/0000-0002-7841-2019

REFERENCES

1. Bowling DR, Egan JE, Hall SJ, Risk DA. Environmental forcing does not induce diel or synoptic variation in the carbon isotope content of forest soil respiration. *Biogeosciences*. 2015;12:5143-5160.
2. Marron N, Plain C, Longdoz B, Epron D. Seasonal and daily time course of the ^{13}C composition in soil CO_2 efflux recorded with a tunable diode laser spectrophotometer (TDLS). *Plant and Soil*. 2009;318:137-151.
3. Moyes AB, Gaines SJ, Siegwolf RTW, Bowling DR. Diffusive fractionation complicates isotopic partitioning of autotrophic and heterotrophic sources of soil respiration: $\delta^{13}C$ of soil respiration. *Plant Cell Environ*. 2010;33:1804-1819.
4. Wingate L, Ogée J, Burlett R, et al. Photosynthetic carbon isotope discrimination and its relationship to the carbon isotope signals of stem, soil and ecosystem respiration. *New Phytol*. 2010;188:576-589.
5. Engel S, Lease HM, McDowell NG, Corbett AH, Wolf BO. The use of tunable diode laser absorption spectroscopy for rapid measurements of the $\delta^{13}C$ of animal breath for physiological and ecological studies. *Rapid Commun Mass Spectrom*. 2009;23:1281-1286.
6. Moyes AB, Schauer AJ, Siegwolf RTW, Bowling DR. An injection method for measuring the carbon isotope content of soil carbon dioxide and soil respiration with a tunable diode laser absorption spectrometer. *Rapid Commun Mass Spectrom*. 2010;24:894-900.
7. Bowling DR, Sargent SD, Tanner BD, Ehleringer JR. Tunable diode laser absorption spectroscopy for stable isotope studies of ecosystem–atmosphere CO_2 exchange. *Agric For Meteorol*. 2003;118:1-19.
8. Talbot JM, Treseder KK. Interactions among lignin, cellulose, and nitrogen drive litter chemistry–decay relationships. *Ecology*. 2012;93:345-354.
9. Melillo JM, Aber JD, Linkins AE, Ricca A, Fry B, Nadelhoffer KJ. Carbon and nitrogen dynamics along the decay continuum: Plant litter to soil organic matter. *Plant and Soil*. 1989;115:189-198.
10. Bollag J-M, Dec J, Huang PM. Formation mechanisms of complex organic structures in soil habitats. In: Sparks DL, ed. *Advances in Agronomy*. New York: Academic Press; 1997:237-266.
11. Marschner B, Brodowski S, Dreves A, et al. How relevant is recalcitrance for the stabilization of organic matter in soils? *J Plant Nutr Soil Sci*. 2008;171:91-110.
12. Grandy AS, Neff JC. Molecular C dynamics downstream: The biochemical decomposition sequence and its impact on soil organic matter structure and function. *Sci Total Environ*. 2008;404:297-307.
13. Schmidt MWI, Torn MS, Abiven S, et al. Persistence of soil organic matter as an ecosystem property. *Nature*. 2011;478:49-56.
14. Huang PM, Wang TSC, Wang MK, Wu MH, Hsu NW. Retention of phenolic acids by noncrystalline hydroxy-aluminum and -iron compounds and clay minerals of soils. *Soil Sci*. 1977;123:213-219.
15. Hernes PJ, Kaiser K, Dyda RY, Cerli C. Molecular trickery in soil organic matter: Hidden lignin. *Environ Sci Technol*. 2013;47:9077-9085.
16. Kirk TK, Connors WJ, Bleam RD, Hackett WF, Zeikus JG. Preparation and microbial decomposition of synthetic [^{14}C]lignins. *Proc Natl Acad Sci*. 1975;72:2515-2519.
17. Haider K, Martin JP. Decomposition in soil of specifically ^{14}C-labeled model and cornstalk lignins and coniferyl alcohol over two years as influenced by drying, rewetting, and additions of an available C substrate. *Soil Biol Biochem*. 1981;13:447-450.
18. Haider K, Trojanowski J. Decomposition of specifically ^{14}C-labelled phenols and dehydropolymers of coniferyl alcohol as models for lignin degradation by soft and white rot fungi. *Arch Microbiol*. 1975;105:33-41.
19. Martin JP, Haider K. Biodegradation of ^{14}C-labeled model and cornstalk lignins, phenols, model phenolase humic polymers, and fungal melanins

as influenced by a readily available carbon source and soil. *Appl Environ Microbiol*. 1979;38:283-289.

20. Hall SJ, Silver WL, Timokhin VI, Hammel KE. Lignin decomposition is sustained under fluctuating redox conditions in humid tropical forest soils. *Glob Change Biol*. 2015;21:2818-2828.
21. Crawford RL. *Lignin Biodegradation and Transformation*. New York: John Wiley; 1981.
22. Kirk TK, Brunow G. Synthetic ^{14}C-labeled lignins. *Methods Enzymol*. 1988;161:65-73.
23. Bowling DR, Burns SP, Conway TJ, Monson RK, White JWC. Extensive observations of CO_2 carbon isotope content in and above a high-elevation subalpine forest. *Global Biogeochem Cycles*. 2005;19: GB3023.
24. R Development Core Team. *R: A Language and Environment for Statistical Computing*. Vienna: R Foundation For Statistical Computing; 2015.
25. Coplen TB. Guidelines and recommended terms for expression of stable-isotope-ratio and gas-ratio measurement results. *Rapid Commun Mass Spectrom*. 2011;25:2538-2560.
26. Hall SJ, Silver WL. Reducing conditions, reactive metals, and their interactions can explain spatial patterns of surface soil carbon in a humid tropical forest. *Biogeochemistry*. 2015;125:149-165.
27. Bowling D, Pataki D, Randerson J. Carbon isotopes in terrestrial ecosystem pools and CO_2 fluxes. *New Phytol*. 2008;178:24-40.
28. Brand WA. High precision isotope ratio monitoring techniques in mass spectrometry. *J Mass Spectrom*. 1996;31:225-235.
29. Crow SE, Sulzman EW, Rugh WD, Bowden RD, Lajtha K. Isotopic analysis of respired CO_2 during decomposition of separated soil organic matter pools. *Soil Biol Biochem*. 2006;38:3279-3291.
30. Torn MS, Davis S, Bird JA, Shaw MR, Conrad ME. Automated analysis of $^{13}C/^{12}C$ ratios in CO_2 and dissolved inorganic carbon for ecological and environmental applications. *Rapid Commun Mass Spectrom*. 2003;17:2675-2682.
31. Berryman EM, Marshall JD, Rahn T, Cook SP, Litvak M. Adaptation of continuous-flow cavity ring-down spectroscopy for batch analysis of $\delta^{13}C$ of CO_2 and comparison with isotope ratio mass spectrometry. *Rapid Commun Mass Spectrom*. 2011;25:2355-2360.
32. Breecker DO, Bergel S, Nadel M, et al. Minor stable carbon isotope fractionation between respired carbon dioxide and bulk soil organic matter during laboratory incubation of topsoil. *Biogeochemistry*. 2015;123:83-98.
33. Ehleringer JR, Buchmann N, Flanagan LB. Carbon isotope ratios in belowground carbon cycle processes. *Ecol Appl*. 2000;10:412-422.
34. Flessa H, Ludwig B, Heil B, Merbach W. The origin of soil organic C, dissolved organic C and respiration in a long-term maize experiment in Halle, Germany, determined by ^{13}C natural abundance. *J Plant Nutr Soil Sci*. 2000;163:157-163.
35. Mueller CW, Gutsch M, Kothieringer K, et al. Bioavailability and isotopic composition of CO_2 released from incubated soil organic matter fractions. *Soil Biol Biochem*. 2014;69:168-178.
36. Šantrůcková H, Bird MI, Lloyd J. Microbial processes and carbon-isotope fractionation in tropical and temperate grassland soils. *Funct Ecol*. 2000;14:108-114.
37. Schweizer M, Fear J, Cadisch G. Isotopic (^{13}C) fractionation during plant residue decomposition and its implications for soil organic matter studies. *Rapid Commun Mass Spectrom*. 1999;13:1284-1290.
38. Boström B, Comstedt D, Ekblad A. Isotope fractionation and ^{13}C enrichment in soil profiles during the decomposition of soil organic matter. *Oecologia*. 2007;153:89-98.
39. Collins HP, Elliott ET, Paustian K, et al. Soil carbon pools and fluxes in long-term corn belt agroecosystems. *Soil Biol Biochem*. 2000;32: 157-168
40. Cusack DF, Chou WW, Yang WH, Harmon ME, Silver WL. Controls on long-term root and leaf litter decomposition in neotropical forests. *Glob Change Biol*. 2009;15:1339-1355.
41. Paul EA, Morris SJ, Bohm S. The determination of soil C pool sizes and turnover rates: Biophysical fractionation and tracers. In: Lal R, Kimble JM, Follett RF, Stewart BA, eds. *Assessment Methods for Soil Carbon*. Boca Raton: CRC Press; 2001:193-206.
42. Hall SJ, McNicol G, Natake T, Silver WL. Large fluxes and rapid turnover of mineral-associated carbon across topographic gradients in a humid tropical forest: Insights from paired ^{14}C analysis. *Biogeosciences*. 2015;12:2471-2487.
43. Hall SJ, Silver WL, Timokhin VI, Hammel KE. Iron addition to soil specifically stabilized lignin. *Soil Biol Biochem*. 2016;98:95-98.
44. Hammel K, Kapich A, Jensen K, Ryan Z. Reactive oxygen species as agents of wood decay by fungi. *Enzyme Microb Technol*. 2002;30: 445-453.
45. Hammel K, Cullen D. Role of fungal peroxidases in biological ligninolysis. *Curr Opin Plant Biol*. 2008;11:349-355.

SUPPORTING INFORMATION

Additional Supporting Information may be found online in the supporting information tab for this article.

How to cite this article: Hall SJ, Huang W, Hammel KE. An optical method for carbon dioxide isotopes and mole fractions in small gas samples: Tracing microbial respiration from soil, litter, and lignin. *Rapid Commun Mass Spectrom*. 2017;31: 1938-1946. https://doi.org/10.1002/rcm.7973